·Article·
Advances in Polar Science
doi: 10.13679/j.advps.2022.0024
March 2023 Vol. 34 No. 1: 28-44

The roles of phosphate in shaping the structure and dynamics of Antarctic soil microbiomes

TAN Jiankang[1†], CAO Huansheng[2†], LIU Li[2], QIN Yiling[3], LIU Feng[3], John CAVA[4], YIN Xiaofei[3], SHEN Jihong[3] & WANG Nengfei[5*]

[1] Department of Ecology and Environment of Lishui, Nanjing 200200, China;
[2] Division of Natural and Applied Sciences, Duke Kunshan University, Suzhou 215316, China;
[3] The First Institute of Oceanography, Ministry of Natural Resources, Qingdao 266061, China;
[4] Center for Fundamental and Applied Microbiomics, Biodesign Institute, Arizona State University, Tempe, AZ 85287, USA;
[5] School of Chemistry and Chemical Engineering, Linyi University, Linyi 276000, China

Received 21 September 2022; accepted 8 February 2023; published online 31 March 2023

Abstract One major consequence of global warming in the Antarctic region is increased ice-free zones. Subsequent colonization of these ice-free areas by penguins alters their biogeochemistry, with one prominent example being elevation of inorganic phosphate concentrations around feces depositions. The complex soil biochemistry in the region makes it difficult to define the causal factors of these changes using common research approaches. Here, we addressed the effects of phosphate alone on microbiome structure and dynamics over time by adding external phosphate to selected soils in the Antarctic region. We then analyzed the soil bacterial community composition and diversity using 16S rRNA amplicon sequencing and compared these data with phosphate levels. Parallel geochemical analysis revealed changes in nine soil geochemical factors upon phosphate addition, all of which were relevant to microbiome structure, with soil pH showing the highest correlation. Links between geochemical factors and composition were identified, as were interactions between bacterial taxa. Additionally, Sphingobacteriia, Sphingobacteriales and Chitinophagaceae were found to be more abundant in phosphate-treated soils. Co-occurrence network analysis revealed significantly increased levels of associations in all major network properties over time after phosphate supplementation. Therefore, we conclude phosphate addition has diverse effects on Antarctic soil microbiomes.

Keywords **phosphate, Antarctic, microbiome composition, network, geochemical factors, ice-free zone**

Citation: Tan J K, Cao H S, Liu L, et al. The roles of phosphate in shaping the structure and dynamics of Antarctic soil microbiomes. Adv Polar Sci, 2023, 34(1): 28-44, doi: 10.13679/j.advps.2022.0024

1 Introduction

Long-term monitoring has shown that Antarctic ice melting is accelerating under global warming (Steig et al., 2009; Rignot et al., 2019). The resulting ice sheet thaw has led to increased amounts of bare soils being exposed during summer (Pritchard et al., 2012; Wang et al., 2016; Nicolas et al., 2017), expanding the pre-existing ice-free ground on the continent (Peck et al., 2005). This has at least two consequences. First, it changes the landscape of Antarctica, connecting these soils to the cycle of local and global biogeochemistry (Cowan et al., 2014). Second, the expanded ice-free zones provide more open ground that is accessible to human activities (Santamans et al., 2017; Convey and Peck, 2019), occupation by local animals

† These authors contributed equally to this work. * Corresponding author, ORCID: 0000-0002-6070-2122, E-mail: wangnengfei@lyu.edu.cn

(Santamans et al., 2017), and inhabitation by nonindigenous microbes (Cannone et al., 2008; Prather et al., 2019).

Colonization by penguins is a prominent external perturbation to expanded ice-free areas (LaRue et al., 2013; Younger et al., 2015) that has several effects. Penguins feeding on sea life form large rookeries on land close to the coasts, which directly impacts the soils in and around the rookeries through physical occupation (Ancel et al., 2017). Additionally, penguin feces dramatically changes the geochemistry and microbiomes of the soils (Santamans et al., 2017; Guo et al., 2018). For example, higher concentrations of heavy metals (e.g., cadmium, copper, arsenic, zinc and selenium) are found in areas receiving penguin feces. The organic contents (e.g., organic carbon and phosphate) and some inorganic elements of soils that receive penguin feces also tend to be higher in rookeries than in surrounding areas (Santamans et al., 2017; Guo et al., 2018). As a result, the microbiomes in these soils have higher proportions of taxa originating from penguin feces (Santamans et al., 2017; Guo et al., 2018). Given the concomitant input of microbial cells and alterations of soil geochemistry, it is difficult to determine the individual effects of the added compounds, nutrients, and toxic metal stressors on the soil microbiome structure.

Among the geochemical factors that are elevated, the concentrations of inorganic phosphate (Pi) are approximately 10-fold higher in rookery soils than in the surrounding soils (Guo et al., 2018). Phosphorus has been found to limit microbial production in polar soils (Darcy et al., 2018; Street et al., 2018). Although some mechanisms of the effects of Pi on soil microbial communities and composition have been proposed (Huang et al., 2016), little is known about the roles that Pi plays in shaping microbiomes in land exposed by melting ice sheets in Antarctica.

In this study, we investigated the effects of Pi on microbial community composition and interactions among constituents in Antarctic soils. To accomplish this, we added external phosphate to three sites on the Fildes Peninsula and observed changes in the soil microbiome over an 11-day study period. During this period, we analyzed relevant geochemical parameters and conducted 16S rRNA gene sequencing followed by network analyses and multivariate correlation analyses to investigate compositional changes and interactions among taxa following phosphate addition.

2 Materials and methods

2.1 Study sites and sample collection

The study area was located on the south coast of the Fildes Peninsula, South Shetland Islands (Figure 1), which is the second largest region of bare soils (Prather et al., 2019). Six plots (S1 to S6) with seemingly homogeneous soil texture were set up in this area (62.22°S, 58.95°W). These six plots formed two similar triangles, with three control plots being the vertices of the inner triangle and the treatment plots being the vertices of the outer triangle. Time 0 samples were collected from both control and treatment plots before phosphate was applied. Immediately after sampling, 270 mL of 0.2 mol·L^{-1} phosphate buffer solution (Na_2HPO_4 : NaH_2PO_4=61 : 39, pH 7 (predetermined for this study site)) was sprayed onto sites S4, S5, and S6 (in the inner triangle) once. All plots were sampled on days 3, 6, and 11.

2.2 Soil geochemical property analyses

Surface soil (top 10 cm) samples were collected from the plots using a sterile garden shovel, placed in sterile plastic storage bags and kept on ice in a cooler during transport to the lab. The samples were stored in a freezer at −20°C upon arrival at the field station lab. Nine soil geochemical properties were measured, moisture content (MC), pH, total organic carbon (TOC), total organic nitrogen (TON) and five soluble nutrients (NH_4^+-N, SiO_3^{2-}-Si, NO_3^--N, NO_2^--N and PO_4^{3-}-P). Samples were dried at 105°C to the same final weight to calculate the MC, which was the proportion of water lost from the wet soil (Schmugge et al., 1980). Soil pH was measured using a pH meter (PHS-3C, Shanghai REX Instrument Factory, Shanghai, China) after adding 10 mL of distilled water to four grams of soil. TOC was measured as previously described (Hu et al., 2012). The soils were then freeze-dried and ground into powder, after which they were treated with 10% HCl and dried before analysis on an element analyzer (EA3000, Euro Vector SpA, Milan, Italy). Soils used to determine nutrients were also freeze-dried and ground, after which water was added at a ratio of 1:10 (g·mL^{-1}). After shaking once every 4 h for 48 h, a nutrient auto-analyzer (QuAAtro, SEAL, Germany) was used to determine other physical and chemical properties, with relative standard deviation less than 5% demonstrated previously (Liu et al., 2016).

2.3 DNA extraction, PCR amplification and sequencing

Genomic DNA was extracted and sequenced as previously described (Guo et al., 2018). Briefly, DNA was extracted from 0.25 g soil samples using a MO BIO PowerSoil DNA Isolation Kit according to the manufacturer's instructions. The v3-v4 region of the 16S rRNA gene was then amplified using primers 806R (5'-GGACTACNNGGGTATCTAAT-3') and 341F (5'-CC TAYGGGRBGCASCAG-3'). Next, amplicons were sequenced on an Illumina MiSeq platform, after which 250-bp paired-end reads were generated. The raw sequence reads were deposited into the NCBI sequencing read archive under accession number SRP218067.

2.4 Sequence analysis

Clean reads were processed and analyzed as previously

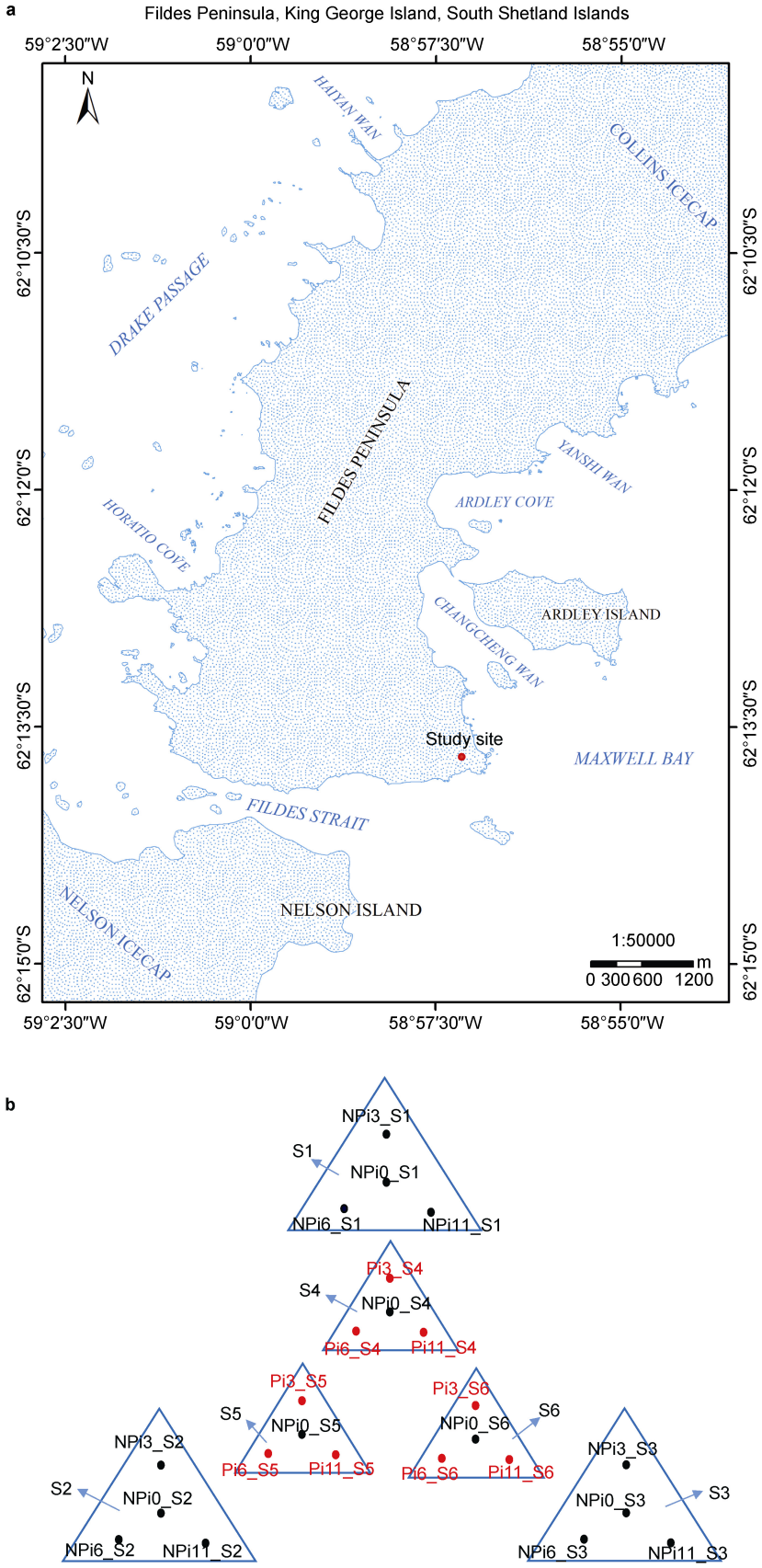

Figure 1 Geographical location (red dots, **a**) and sampling sites (**b**) on the south coast of Antarctica.

described (Guo et al., 2018). Briefly, filtered reads were assembled and clustered into operational taxonomical units (OTUs) at a 97% identity cutoff using UPARSE 7.0 (Edgar, 2013). The most frequent sequence for an OTU was selected as the representative sequence of the OTU. The species were annotated and analyzed against the representative sequence of the OTUs using QIIME 19.1 and the SSU rRNA database (Quast et al., 2013) of SILVA (Version 128) (Wang et al., 2007) to obtain the taxonomic information and calculate abundance at each classification level for all samples. Finally, all samples were normalized at the same sequence depth (51249 reads) for the subsequent alpha and beta diversity analysis.

2.5 Statistical analysis

Statistical analyses of the alpha diversity of soil samples, Chao1, Good's coverage, ACE, and Shannon's index (H') were performed using QIIME 1.9.1 (Caporaso et al., 2010). The species accumulation box-plot was generated using the R program (version 3.4.4) (R Core Team, 2008) to check if the sampling efforts were sufficient so as to reflect the species present at the study sites. A linear discriminant analysis effect size (LEfSe) tool was used to identify the biomarker taxa abundance between study sites and timepoints (Segata et al., 2011), which was also verified by one-way ANOVA followed by Tukey's test. The relevance of environmental factors associated with the distribution patterns of bacterial communities of the samples was analyzed by Bray-Curtis distance-based redundancy analysis (db-RDA) using the R vegan package (Dixon, 2003). We used network analysis to identify associations between geochemical parameters and specific microbial modules (subnetworks of OTUs) as described by Guidi et al. (2016). Specifically, we correlated each OTU with seven of nine geochemical parameters using sparse partial least squares (sPLS) regression (Shen and Huang, 2008) as implemented in the R mixOmics package (Rohart et al., 2017). The global scale-free network of OTUs based on the relative abundance of all samples was then constructed, after which modules were identified using the R WGCNA package (Langfelder and Horvath, 2008). Finally, the modules were correlated with geochemical parameters across all samples using Spearman's correlation, as previously described (Guo et al., 2018).

3 Results

3.1 Geochemical properties of soils

The soil Pi content in sites with phosphate application was changed compared with that of the control sites (Figure 2 and Table S1). Interestingly, the Pi content in the treatments rose to peak values on day 6, then declined, while two of the three controls showed a similar trend, but to a much lesser degree. Repeated-measures ANOVA and the Kruskal Wallis test revealed no significant changes over time for the other eight metrics (Figures 2a–2i). However, some of the factors (e.g., TOC, TON, NO_3^--N) did show noticeable variations, although these changes were not statistically significant (Kruskal Wallis test, P>0.05). These findings

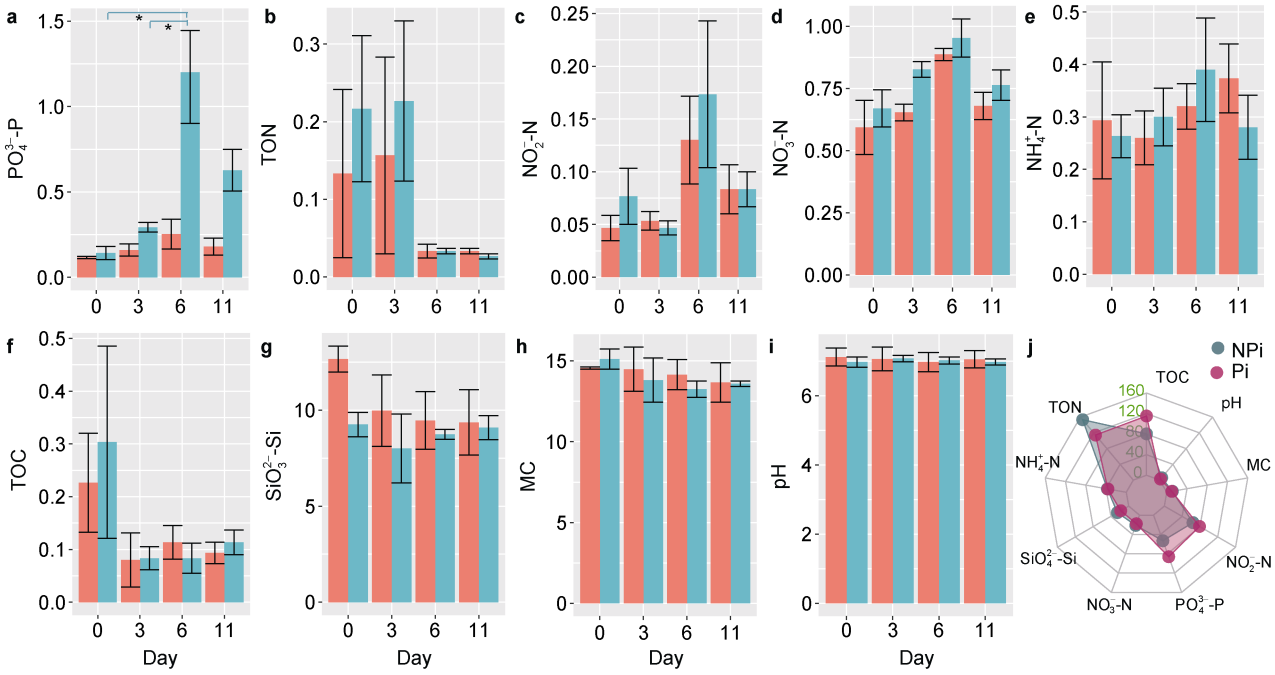

Figure 2 Soil geochemical factors and their variations with time in terms of coefficients of variation. **a–i**, Geochemical factors; *: significance at 0.05 level between time points of Pi treatment; The orange bars represent the controls, the green bars represent the treatments; **j**, Web plot of the coefficients of variation of all nine geochemical factors.

suggest that there are high variations and heterogeneities in soil texture, even across small study areas. Consistent with this inference, the coefficients of variations (CVs) for the controls and treatments were both high, particularly for TOC, TON, NO_2^--N, and NO_3^--N, while the remaining factors showed smaller CVs (Figure 2j).

3.2 Bacterial diversity and community composition

A total of 1665740 raw reads were obtained, giving rise to 1551364 clean reads after processing. Overall, there was an average of 62054 reads per sample, leading to more than 1800 OTUs for each sample (Table S2). Among the six study sites and four time points, NPi11_S1 (NPi: no Pi added; 11: day 11; S1: control site 1; see naming details in Table S1) contained the most OTUs (2840) while NPi0_S1 contained the least (1848). The Good's coverage estimator of the OTUs in the samples ranged from 0.978 to 0.989, indicating that the sequences adequately covered most of the bacterial diversity in all samples. The Chao1 and AEC values of NPi0_S1 were lowest among the 12 samples. The species accumulation boxplot (Figure S1) was saturated with all 24 samples, implying the species diversity of the study sites was adequately represented by these samples.

We used four approaches to study the effects of phosphate addition on soil microbiome composition. First, we examined clustering of the samples based on the relative abundance of OTUs they contained. As shown in Figure 3a, the control samples from the same sites tended to cluster together over time and were separate from those of other sites. Within each site, the samples were also separated according to sampling times. For example, samples collected on day 0 and 11 were furthest apart, while those from day 3 and 6 were closer to each other. In contrast, the clustering of the samples in the treatments led to a slightly

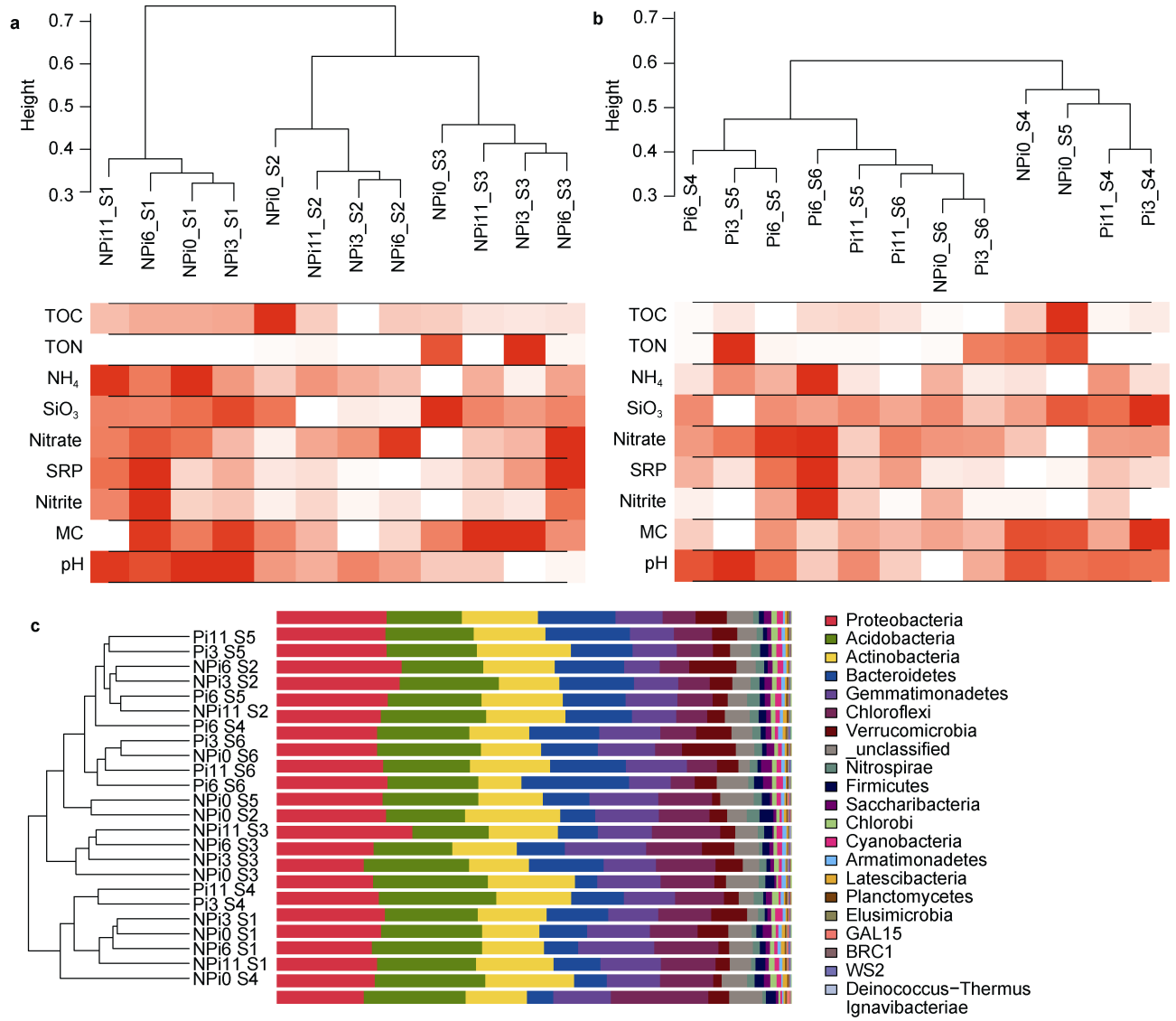

Figure 3 The clustering of OTU abundance in the samples in NPi and Pi treatments. **a**, The clustering of the NPi treatments; **b**, The clustering of Pi treatments; **c**, The top taxa of all samples. The height on the *y*-axis represents the distance between the samples.

different pattern (Figure 3b). For example, with the exception of one S5 sample that joined the S6 samples, the samples collected from Sites S4 and S5 were clustered into two groups. This overall difference between the controls and treatments suggested that phosphate had some effect on the microbiome composition.

Next we examined the taxonomical differences between the controls and treatments. Among the 24 samples, the OTUs were mapped to more than 40 phyla, the most abundant being Proteobacteria (20.54%), Acidobacteria (18.23%), Actinobacteria (13.84%), Bacteroidetes (11.13%), Gemmatimonadetes (10.74%), Chloroflexi (9.01%), Verrucomicrobia (4.50%), and Nitrospirae (1.43%). Similarities between samples could be seen from the UPGMA clusters. Based on the taxa and their abundance, sample clustering was affected by both the vicinity and timing of sampling (Figure 3c). When examined together, samples collected from within the same sites had higher similarities for some sites, such as non-phosphate treated site S1 (i.e., NPi0_S1, NPi3_S1, NPi6_S1, NPi11_S1), S3 (NPi0_S3, NPi3_S3, NPi6_S3, NPi11_S3), and S6 (NPi0_S6, Pi3_S6, Pi6_S6, Pi11_S6). Additionally, similarity associated with location vicinity was also observed between S1 and S4, S2 and S5, and S3 and S6. These findings suggest that the effects of Pi addition were not sufficient to obscure soil heterogeneity among study sites.

Finally, we compared the effects of phosphate addition on some specific taxa. Based on the LEfSe, 24 taxa showed LDA scores greater than 3 (the cutoff for significance; Figure 4a and Table S3). Group 6, which contained samples from phosphate-added soils collected on day 6, was found to have the most enriched taxa. Specifically, 12 out of 24 (50%) taxa were more abundant than at other sites at the same time, including some classes, orders, and families of the phylum Bacteroidetes. These findings also indicated that soil microbes in this polar region could respond to phosphate supplementation within six days.

3.3 Correlations between geochemical factors and bacterial community structure

Phosphate supplementation can change microbiome composition directly by causing differential growth of bacterial species and indirectly by altering other geochemical factors. Here, the indirect effects appeared to be marginal, although they could certainly be factor specific. Given that the solution we applied was also an effective pH buffer, pH and MC remained unchanged as expected, while other geochemical factors (carbon, nitrogen, and silicon) showed statistically insignificant variations.

Based on the above findings, we investigated the direct effects of Pi on microbiome composition. Correlation analysis conducted using the first principal component RDA1 method (Table 1) indicated that pH (R^2 = 0.667, P < 0.001) was the factor most closely correlated with bacterial community composition at the study sites. Additionally, MC (R^2 = 0.467, P < 0.003) and SiO_3^{2-}-Si (R^2 = 0.561, P < 0.003) were the most similar in structure among these study sites, followed by TON (R^2 = 0.410, P < 0.01), NO_3^--N (R^2 =0.280, P <0.05) and PO_4^{3-}-P (R^2 = 0.243, P < 0.05). Moreover, orders and families belonging to the class Sphingobacteriia were significantly associated with phosphate and were more abundant in soils with added phosphate than those without (Figure 4a).

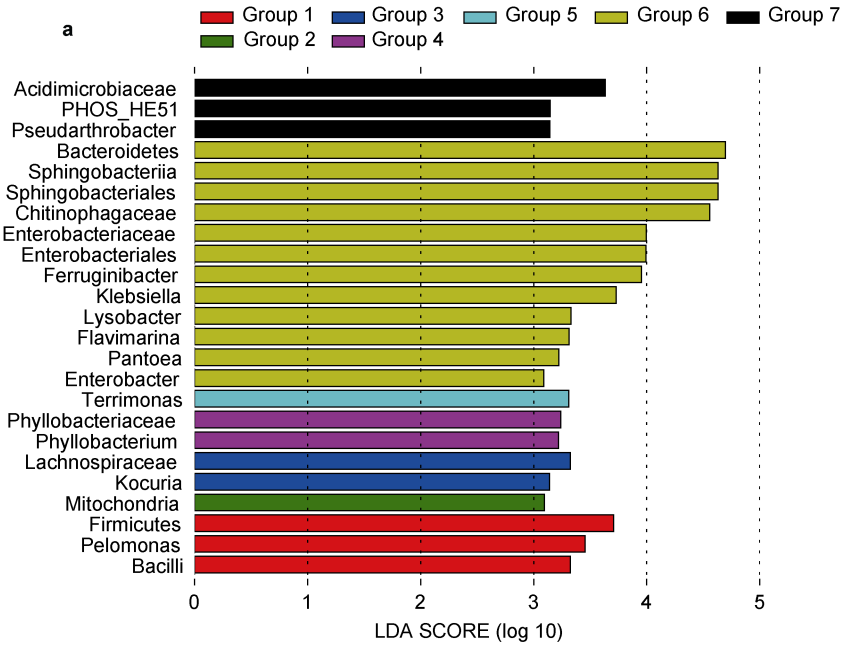

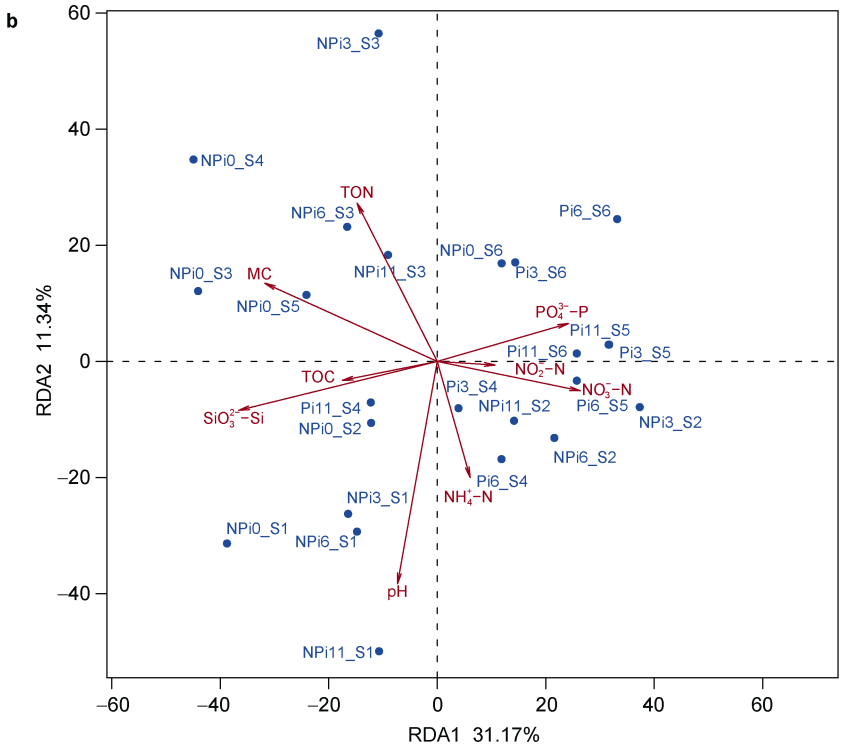

Figure 4 The taxa showing different relative abundance among sites based on the LDA score (**a**) and Canonical correspondence analysis conducted to show correlations between bacterial communities and environmental factors of 24 samples from four sampling sites (**b**).

Table 1 The association of the factors with microbiome composition revealed by redundancy analysis

	RDA1	RDA2	R^2	Pr(>*r*)
TOC	–0.974	–0.227	0.124	0.249
TON	–0.419	0.908	0.408	0.008
NH_4^+-N	0.241	–0.970	0.190	0.091
SiO_3^{2-}-Si	–0.962	–0.272	0.557	0.003
NO_3^--N	0.981	–0.195	0.280	0.033
PO_4^{3-}-P	0.950	0.312	0.249	0.042
NO_2^--N	0.999	–0.046	0.044	0.626
MC	–0.906	0.423	0.466	0.002
pH	–0.182	–0.983	0.676	0.001

3.4 Effects of phosphate supplementation on the interactions between taxa and between modules and geochemical factors

We used a co-occurrence network to show the network properties of microbiome composition at different levels. Tighter associations among the taxa/OTUs were observed after Pi addition, with the Pi microbiome network having 20 modules and the NPi control network only having 12 modules (Figure 5). These findings suggest that Pi supplementation caused OTUs to be more 'locally' connected. Fewer (11 versus 14) modules that were geochemically correlated (P<0.05) were found under Pi than NPi. Specifically, more modules were correlated with TOC, TON, MC, and pH under Pi treatment than those were correlated with ammonia. Moreover, the values of the correlation and significance were higher in the Pi treatments in most cases. These findings represent additional evidence of the responses of microbiomes to Pi supplementation. We used the geochemical factor PO_4^{3-}-P (SRP) as an example module to show the correlations between OTUs (Figure S2). We then examined the connectivity between OTUs within the detected modules. For this comparison, we selected modules showing similar patterns of correlation to geochemical factors under either condition, such as the NPi (grey) and the Pi (pink) modules (Figure 6). The OTUs from these Pi treated modules were more densely interconnected than those from the NPi treated modules, as demonstrated by the presence of eight network parameters, e.g., node degree or shortest path length (Figure S3).

Finally, we checked whether the dominant taxa identified were also hub nodes in the modules (subnetworks) identified above. To address this question, we created an OTU table of taxa (instead of OTU IDs) for Pi and NPi samples and conducted network analysis separately to identify modules of taxa. For Pi, we found 19% of the dominant taxa also appeared in these modules, whereas only 0.6% of the dominant taxa appeared in NPi modules. This further confirmed the finding above that phosphate supplementation changed the associations between microorganisms in soil microbiomes. We also determined whether the dominant taxa were hub nodes under either

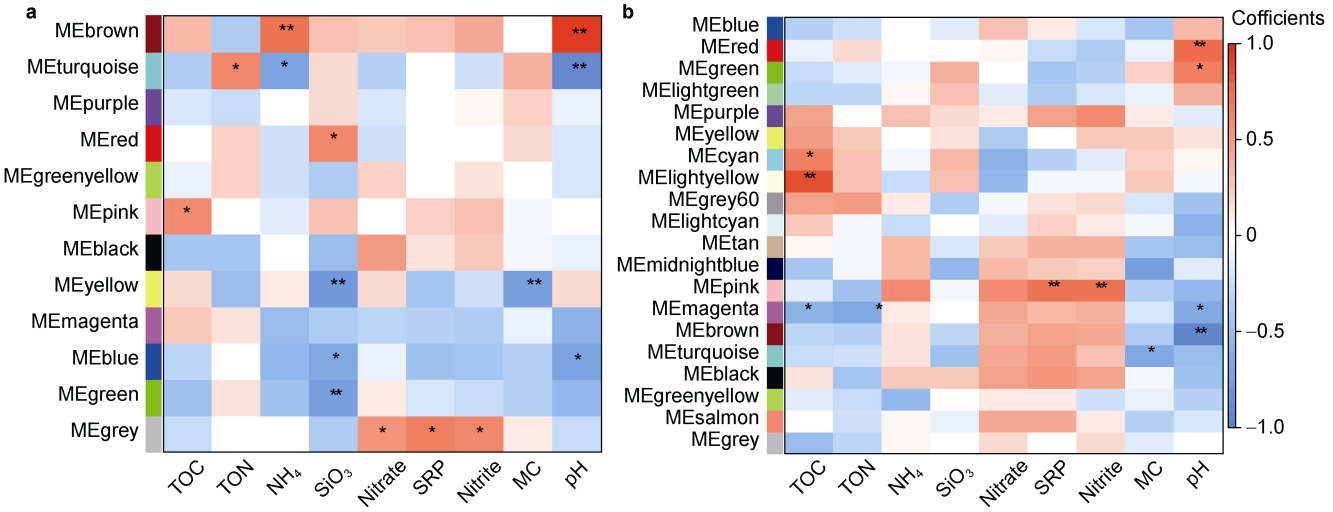

Figure 5 The modules identified in the co-occurrence networks of microbiomes with phosphate addition (**a**) and without phosphate addition (**b**). The * and ** represent P <0.05 and P < 0.01 level of test significance of each module with geochemical factors (column names), respectively. The scale bar on the right represents the range of the correlation coefficients.

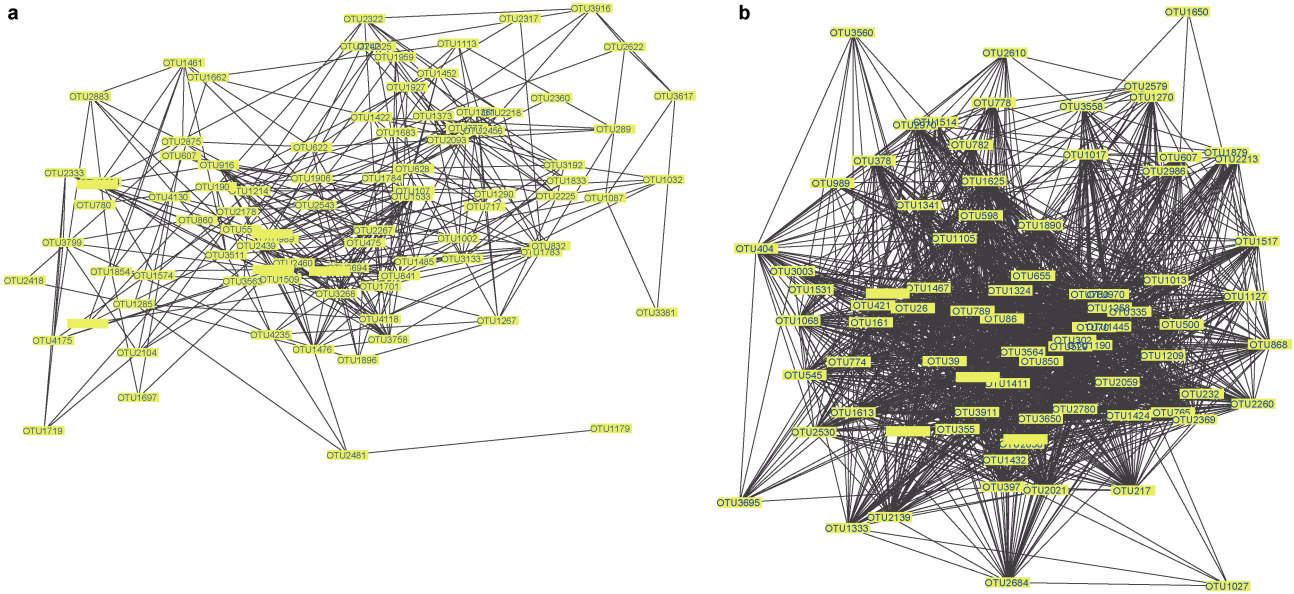

Figure 6 The network topology between NPi (grey; **a**) and Pi (pink; **b**) modules.

condition. We defined a hub node as a taxon that is in the top 25% of the most connected nodes. From this analysis we found that 5% of the dominant taxa were hub nodes in Pi, whereas 6% of the dominant taxa were hub nodes in NPi. Some of the hub nodes are listed in Table S4. These hubs only partially overlap between NPi and Pi (Figure S4 and Table S4). Here, we present one example of the hub nodes in the Pi treatments. The OTUs of the class Sphingobacteriia (a hub taxon) varied in abundance with soil Pi content (increasing first then declining), while the most abundant OTU was in the family Chitinophagaceae (Figure S5). This suggests that phosphate supplementation affects the microbiome composition by increasing the abundance of non-dominant taxa rather than increasing the abundance of taxa that were already dominant before supplementation.

4 Discussion

We identified the effects of phosphate on microbiome composition to distinguish the indirect impact of penguin feces in bare soils from the overall effects. Treatment with Pi increased variations in geochemical factors, changed the abundances of some taxa, and increased the interactions among taxa, resulting in more connected soil communities. Given that these bare soils are connected to local biogeochemistry, penguin activities are an important factor that can play a major role in development of soil microbiomes via an influx of Pi (Santamans et al., 2017;

Guo et al., 2018).

Similarities and differences were found between the effects of penguin feces and phosphate alone. Pi and feces both changed the soil Pi content, but not pH, while the rest of the geochemical factors were only changed by feces (Guo et al., 2018). Additionally, both Pi and feces changed the composition, but not the diversity of the microbiome. For example, some taxa such as Sphingobacteriia, which was a hub taxon in the network modules, were enriched in presence of both feces and Pi. Finally, soil moisture differed between the controls and treatments in response to feces, but not under Pi supplementation. These findings suggest that physical water retention is important to the microbiome structure.

Phosphate is an important and often limiting factor in soils, including polar soils (Teixeira et al., 2010; Shen et al., 2011). Recently, several studies have investigated the importance of Pi in shaping microbiome composition in various environments, including humans, rats, and soils (Richardson and Simpson, 2011; Castrillo et al., 2017; Lau et al., 2018; Miao et al., 2018; Finkel et al., 2019; Gumiere et al., 2019). One common feature is that Pi is associated with some taxa. For example, 14 genera were found to be positively correlated with Pi in the gut microbiota of hemodialysis patients (Miao et al., 2018). Furthermore, different sources of phosphorus have been found to cause different soil microbial interactions (Gumiere et al., 2019). Pi has also been shown to act as an important regulator of microbiome structure. Although still preliminary, mechanistic research has shown that some microbiomes can degrade phytate to release phosphate for plants (Shulse et al., 2019). Another study showed that the changes in rat gut microbiomes caused by Pi might be associated with ferric citrate, a phosphate binder (Lau et al., 2018).

One important finding of the present study is that Pi increases the interactions among taxa. This effect was also observed in sugarcane soil microbiomes, and the degree of the effects was found to vary with the source of the Pi used (Gumiere et al., 2019). In addition to increased bacterial interactions, decreased fungal interactions were observed in this study. One prominent example of the increased interactions is the class Sphingobacteriia, which is a hub taxon highly connected to other taxa that varies in abundance as soil Pi content changes. The increased interactions manifest in network properties such as node degree of connectivity and shortest path length for each node.

In this study, we observed that the soil microbial composition of phosphate-supplemented samples changed between study sites (Kuramae et al., 2012; Huang et al., 2016) and temporally. Bacteroidetes, Sphingobacteriia, Sphingobacteriales, and Chitinophagaceae were found to be more abundant in phosphate treated soil samples than in control samples. Moreover, db-RDA analysis showed that in the plot of the analysis only Pi11_S4 was on the left side of the phosphate origin in nine soil samples from areas treated with phosphate.

This study also showed that soil microbial composition was positively correlated with soil pH, which is in accordance with the results of previous studies (Wang et al., 2015). Aciego Pietri and Brookes (2008) also concluded that soil pH had marked effects on microbial biomass by affecting the availability of biologically toxic Al and organic C solubility. Interestingly, the orders, families, and classes of the phylum Gemmatimonadete were significantly associated with phosphate. Overall, these results imply that soil pH may be another factor influencing soil.

Phosphate also increases C utilization by soil microbes, which ultimately improves soil microbial biomass and changes the community composition (Liu et al., 2012; Li et al., 2015). Relieved Pi constraint and changes in soil pH and osmotic potential after Pi addition can also influence microbial growth (Thirukkumaran and Parkinson, 2000; Liu et al., 2013). Regardless of the route, Pi supplementation eventually affects phosphate in the soil. We found that the abundance of the orders and families of the class Sphingobacteriia in phosphate-treated soils increased significantly and were correlated with phosphate content, which also confirms that the addition of phosphate affects soil bacterial communities and diversity. The phosphate concentration in soil initially rose slowly over time, then increased quickly to its highest level, after which it decreased in plots S4, S5 and S6. The changes in Sphingobacteriia in soil over time were consistent with those of the phosphate content at the same study sites. Sphingobacteriia can use phosphorus to produce sphingomyelin, so the richness of Sphingobacteriia increased because of increases in the soil phosphate content (Kämpfer, 2015). In addition to pH and phosphate, MC was found to influence the soil bacterial communities. Soil moisture is another main driver of soil C and N transformations in soils. This is because soil moisture affects microbial activity and survival, and decreases in water content are known to lead to decreased connectivity between substrates and microorganisms (Chenu et al., 2014).

With global climate change, bare soils in Antarctic coastal areas during summer are increasing. Penguins are the dominant animals in these areas, and the phosphate content of penguin feces is high (Zhu et al., 2014). Amphibian penguins bring phosphorus from marine life to the land through diet and excretion, causing changes in soil bacterial communities (Sandoval-Motta et al., 2017). Therefore, the results presented herein also shed light on the ocean-land phosphate transfer and the effects of such transfer on nearshore soil microorganisms.

5 Conclusions

By adding external phosphate to soils in the Antarctic region, we demonstrated that the effects of increased phosphate are reflected in both soil geochemistry and bacterial microbiome composition. Most prominently, added phosphate increased the associations among taxa in

the soil microbiome. Moreover, some of the taxa showing the greatest changes in relative abundance were also hub nodes in network modules. These changes in composition were also found to be correlated with geochemical factors such as SRP, which was consistent with the results of network analysis. Therefore, the effects of phosphate additions are more general (working on many taxa) than specific (working on a few specific taxa).

Acknowledgments This research was funded by the National Key R&D Program of China (Grant no. 2018YFC1406700), the National Natural Science Foundation of China (Grant no. 41776198) and the Basic Scientific Fund for National Public Research Institutes of China (Grant no. GY0219Q10). We thank two anonymous reviewers for providing the valuable reviewing comments and suggestions on this manuscript.

References

Aciego Pietri J C, Brookes P C. 2008. Relationships between soil pH and microbial properties in a UK arable soil. Soil Biol Biochem, 40(7): 1856-1861, doi:10.1016/j.soilbio.2008.03.020.

Ancel A, Cristofari R, Trathan P N, et al. 2017. Looking for new emperor penguin colonies? Filling the gaps. Glob Ecol Conserv, 9: 171-179, doi:10.1016/j.gecco. 2017.01.003.

Cannone N, Wagner D, Hubberten H W, et al. 2008. Biotic and abiotic factors influencing soil properties across a latitudinal gradient in Victoria Land, Antarctica. Geoderma, 144(1/2): 50-65, doi:10.1016/j.geoderma.2007.10.008.

Caporaso J G, Kuczynski J, Stombaugh J, et al. 2010. QIIME allows analysis of high-throughput community sequencing data. Nat Methods, 7(5): 335-336, doi:10.1038/nmeth.f.303.

Castrillo G, Teixeira P J P L, Paredes S H, et al. 2017. Root microbiota drive direct integration of phosphate stress and immunity. Nature, 543(7646): 513-518, doi:10.1038/nature21417.

Chenu C, Garnier P, Monga O, et al. 2014. Predicting the response of soil organic matter microbial decomposition to moisture. EGU General Assembly 2014. Vienne, Austria: European Geosciences Union.

Convey P, Peck L S. 2019. Antarctic environmental change and biological responses. Sci Adv, 5(11): eaaz0888, doi:10.1126/sciadv.aaz0888.

Cowan D A, Makhalanyane T P, Dennis P G, et al. 2014. Microbial ecology and biogeochemistry of continental Antarctic soils. Front Microbiol, 5: 154, doi:10.3389/fmicb.2014.00154.

Darcy J L, Schmidt S K, Knelman J E, et al. 2018. Phosphorus, not nitrogen, limits plants and microbial primary producers following glacial retreat. Sci Adv, 4(5): eaaq0942, doi:10.1126/sciadv.aaq0942.

Dixon P. 2003. VEGAN, a package of R functions for community ecology. J Veg Sci, 14(6): 927-930, doi:10.1111/j.1654-1103.2003.tb02228.x.

Edgar R C. 2013. UPARSE: highly accurate OTU sequences from microbial amplicon reads. Nat Methods, 10(10): 996-998, doi:10.1038/nmeth.2604.

Finkel O M, Salas-González I, Castrillo G, et al. 2019. The effects of soil phosphorus content on plant microbiota are driven by the plant phosphate starvation response. PLoS Biol, 17(11): e3000534, doi:10.1371/journal.pbio.3000534.

Guidi L, Chaffron S, Bittner L, et al. 2016. Plankton networks driving carbon export in the oligotrophic ocean. Nature, 532(7600): 465-470, doi:10.1038/nature16942.

Gumiere T, Rousseau A N, da Costa D P, et al. 2019. Phosphorus source driving the soil microbial interactions and improving sugarcane development. Sci Rep, 9(1): 4400, doi:10.1038/s41598-019-40910-1.

Guo Y D, Wang N F, Li G Y, et al. 2018. Direct and indirect effects of penguin feces on microbiomes in Antarctic ornithogenic soils. Front Microbiol, 9: 552, doi:10.3389/fmicb.2018.00552.

Hu L M, Shi X F, Yu Z G, et al. 2012. Distribution of sedimentary organic matter in estuarine–inner shelf regions of the East China Sea: Implications for hydrodynamic forces and anthropogenic impact. Mar Chem, 142-144: 29-40, doi:10.1016/j.marchem.2012.08.004.

Huang J S, Hu B, Qi K B, et al. 2016. Effects of phosphorus addition on soil microbial biomass and community composition in a subalpine spruce plantation. Eur J Soil Biol, 72: 35-41, doi:10.1016/j.ejsobi.2015. 12.007.

Kämpfer P. 2015. Sphingobacteriia class. nov. Bergey's manual of systematics of archaea and bacteria, doi:10.1002/9781118960608. cbm00013.

Kuramae E E, Yergeau E, Wong L C, et al. 2012. Soil characteristics more strongly influence soil bacterial communities than land-use type. FEMS Microbiol Ecol, 79(1): 12-24, doi:10.1111/j.1574-6941.2011.01192.x.

Langfelder P, Horvath S. 2008. WGCNA: an R package for weighted correlation network analysis. BMC Bioinform, 9: 559, doi:10.1186/1471-2105-9-559.

LaRue M A, Ainley D G, Swanson M, et al. 2013. Climate change winners: receding ice fields facilitate colony expansion and altered dynamics in an Adélie penguin metapopulation. PLoS One, 8(4): e60568, doi:10.1371/journal.pone.0060568.

Lau W L, Vaziri N D, Nunes A C F, et al. 2018. The phosphate binder ferric citrate alters the gut microbiome in rats with chronic kidney disease. J Pharmacol Exp Ther, 367(3): 452-460, doi:10.1124/jpet. 118.251389.

Li J, Li Z A, Wang F M, et al. 2015. Effects of nitrogen and phosphorus addition on soil microbial community in a secondary tropical forest of China. Biol Fertil Soils, 51(2): 207-215, doi:10.1007/s00374-014-0964-1.

Liu J, Zang J Y, Zhao C Y, et al. 2016. Phosphorus speciation, transformation, and preservation in the coastal area of Rushan Bay. Sci Total Environ, 565: 258-270, doi:10.1016/j.scitotenv.2016.04.177.

Liu L, Gundersen P, Zhang T, et al. 2012. Effects of phosphorus addition on soil microbial biomass and community composition in three forest types in tropical China. Soil Biol Biochem, 44(1): 31-38, doi:10.1016/j.soilbio.2011.08.017.

Liu L, Zhang T, Gilliam F S, et al. 2013. Interactive effects of nitrogen and phosphorus on soil microbial communities in a tropical forest. PLoS One, 8(4): e61188, doi:10.1371/journal.pone.0061188.

Miao Y Y, Xu C M, Xia M, et al. 2018. Relationship between gut microbiota and phosphorus metabolism in hemodialysis patients: a preliminary exploration. Chin Med J, 131(23): 2792-2799, doi:10.4103/0366-6999.246059.

Nicolas J P, Vogelmann A M, Scott R C, et al. 2017. January 2016 extensive summer melt in West Antarctica favoured by strong El Niño. Nat Commun, 8: 15799, doi:10.1038/ncomms15799.

Peck L S, Clark M S, Clarke A, et al. 2005. Genomics: applications to Antarctic ecosystems. Polar Biol, 28(5): 351-365, doi:10.1007/s 00300-004-0671-8.

Prather H M, Casanova-Katny A, Clements A F, et al. 2019.

Species-specific effects of passive warming in an Antarctic moss system. R Soc Open Sci, 6(11): 190744, doi:10.1098/rsos.190744.

Pritchard H D, Ligtenberg S M, Fricker H A, et al. 2012. Antarctic ice-sheet loss driven by basal melting of ice shelves. Nature, 484(7395): 502-505, doi:10.1038/nature10968.

Quast C, Pruesse E, Yilmaz P, et al. 2013. The SILVA ribosomal RNA gene database project: improved data processing and web-based tools. Nucleic Acids Res, 41 (Database issue): D590-D596, doi:10.1093/nar/gks1219.

Richardson A E, Simpson R J. 2011. Soil microorganisms mediating phosphorus availability update on microbial phosphorus. Plant Physiol, 156(3): 989-996, doi:10.1104/pp.111.175448.

Rignot E, Mouginot J, Scheuchl B, et al. 2019. Four decades of Antarctic Ice Sheet mass balance from 1979–2017. Proc Natl Acad Sci USA, 116(4): 1095-1103, doi:10.1073/pnas.1812883116.

Rohart F, Gautier B, Singh A, et al. 2017. mixOmics: an R package for 'omics feature selection and multiple data integration. PLoS Comput Biol, 13(11): e1005752, doi:10.1371/journal.pcbi.1005752.

Sandoval-Motta S, Aldana M, Frank A. 2017. Evolving ecosystems: inheritance and selection in the light of the microbiome. Arch Med Res, 48(8): 780-789, doi:10.1016/j.arcmed.2018.01.002.

Santamans A C, Boluda R, Picazo A, et al. 2017. Soil features in rookeries of Antarctic penguins reveal sea to land biotransport of chemical pollutants. PLoS One, 12(8): e0181901, doi:10.1371/journal.pone. 0181901.

Schmugge T J, Jackson T J, McKim H L. 1980. Survey of methods for soil moisture determination. Water Resour Res, 16(6): 961-979, doi:10.1029/wr016i006p00961.

Segata N, Izard J, Waldron L, et al. 2011. Metagenomic biomarker discovery and explanation. Genome Biol, 12(6): R60, doi:10.1186/gb- 2011-12-6-r60.

Shen H P, Huang J Z. 2008. Sparse principal component analysis via regularized low rank matrix approximation. J Multivar Anal, 99(6): 1015-1034, doi:10.1016/j.jmva.2007.06.007.

Shen J B, Yuan L X, Zhang J L, et al. 2011. Phosphorus dynamics: from soil to plant. Plant Physiol, 156(3): 997-1005, doi:10.1104/pp.111.175232.

Shulse C N, Chovatia M, Agosto C, et al. 2019. Engineered root bacteria release plant-available phosphate from phytate. Appl Environ Microbiol, 85(18): e01210-e01219, doi:10.1128/AEM.01210-19.

Steig E J, Schneider D P, Rutherford S D, et al. 2009. Warming of the Antarctic ice-sheet surface since the 1957 International Geophysical Year. Nature, 457(7228): 459-462, doi:10.1038/nature07669.

Street L E, Mielke N, Woodin S J. 2018. Phosphorus availability determines the response of tundra ecosystem carbon stocks to nitrogen enrichment. Ecosystems, 21(6): 1155-1167, doi:10.1007/s10021-017-0209-x.

Teixeira L C R S, Peixoto R S, Cury J C, et al. 2010. Bacterial diversity in rhizosphere soil from Antarctic vascular plants of Admiralty Bay, maritime Antarctica. ISME J, 4(8): 989-1001, doi:10.1038/ismej.2010.35.

The R Development Core Team (R Core Team). 2014. R: a language and environment for statistical computing. MSOR connections, 2014(1).

Thirukkumaran C M, Parkinson D. 2000. Microbial respiration, biomass, metabolic quotient and litter decomposition in a lodgepole pine forest floor amended with nitrogen and phosphorous fertilizers. Soil Biol Biochem, 32(1): 59-66, doi:10.1016/S0038-0717(99)00129-7.

Wang N F, Zhang T, Zhang F, et al. 2015. Diversity and structure of soil bacterial communities in the Fildes Region (maritime Antarctica) as revealed by 454 pyrosequencing. Front Microbiol, 6: 1188, doi:10.3389/fmicb.2015.01188.

Wang N F, Zhang T, Yang X, et al. 2016. Diversity and composition of bacterial community in soils and lake sediments from an Arctic lake area. Front Microbiol, 7: 1170, doi:10.3389/fmicb.2016.01170.

Wang Q, Garrity G M, Tiedje J M, et al. 2007. Naive Bayesian classifier for rapid assignment of rRNA sequences into the new bacterial taxonomy. Appl Environ Microbiol, 73(16): 5261-5267, doi:10.1128/AEM.00062-07.

Younger J, Emmerson L, Southwell C, et al. 2015. Proliferation of East Antarctic Adélie penguins in response to historical deglaciation. BMC Evol Biol, 15: 236, doi:10.1186/s12862-015-0502-2.

Zhu R B, Wang Q, Ding W, et al. 2014. Penguins significantly increased phosphine formation and phosphorus contribution in maritime Antarctic soils. Sci Rep, 4: 7055, doi:10.1038/srep07055.

Supplementary Figures and Tables

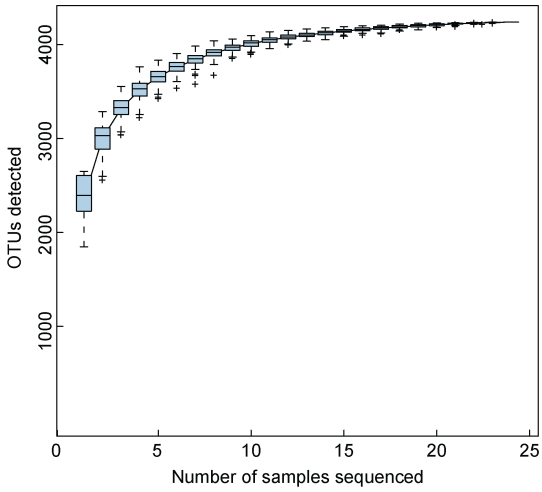

Figure S1 The taxon accumulation curve.

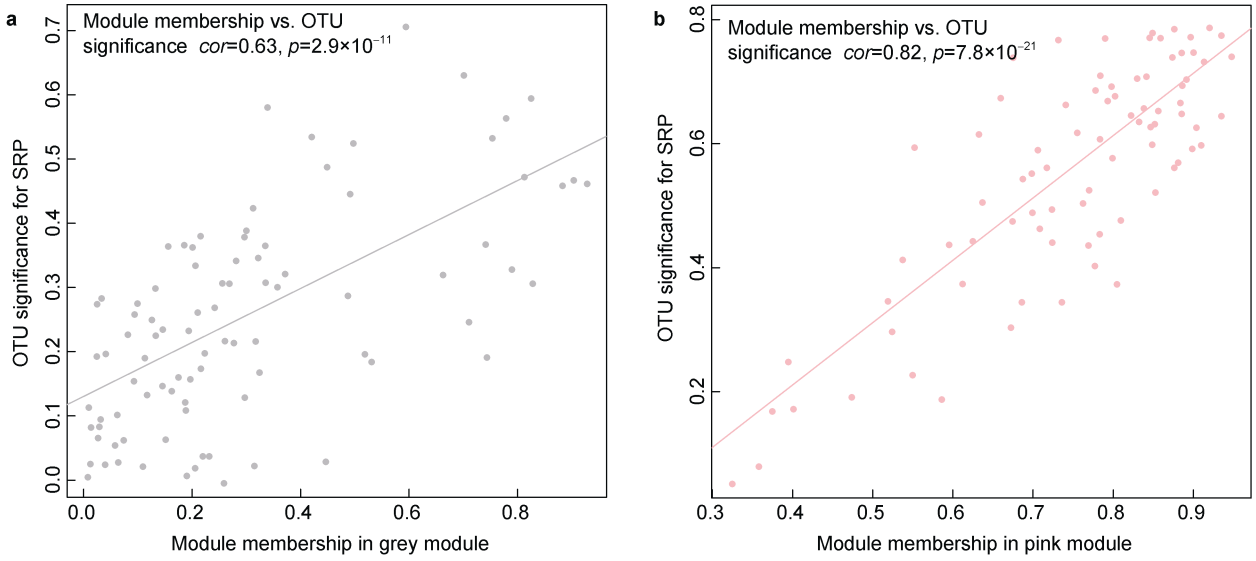

Figure S2 The regression between the OTU module membership and OTU significance for SRP. **a**, NPi sample; **b**, The Pi treatments.

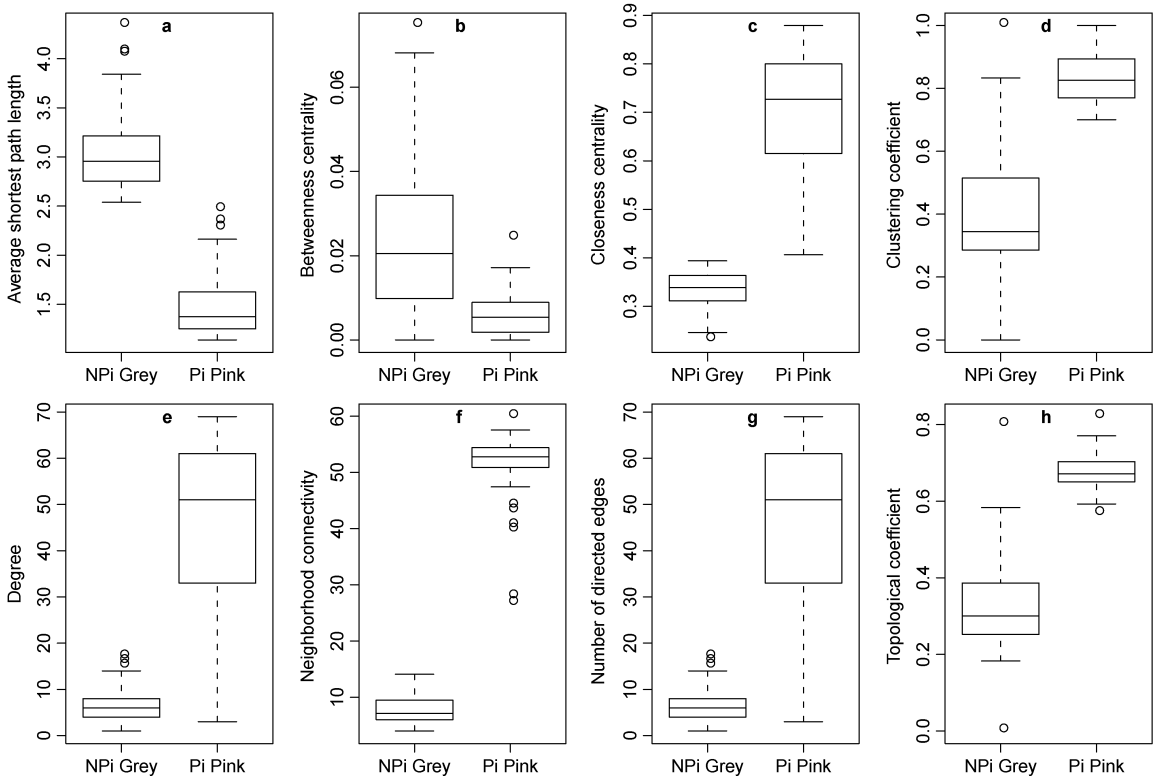

Figure S3 The comparison of the network properties of the Grey and Pink modules.

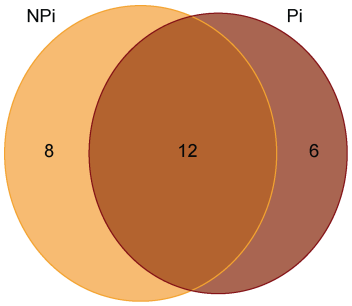

Figure S4 The Venn diagram of the hub taxa between NPi and Pi conditions.

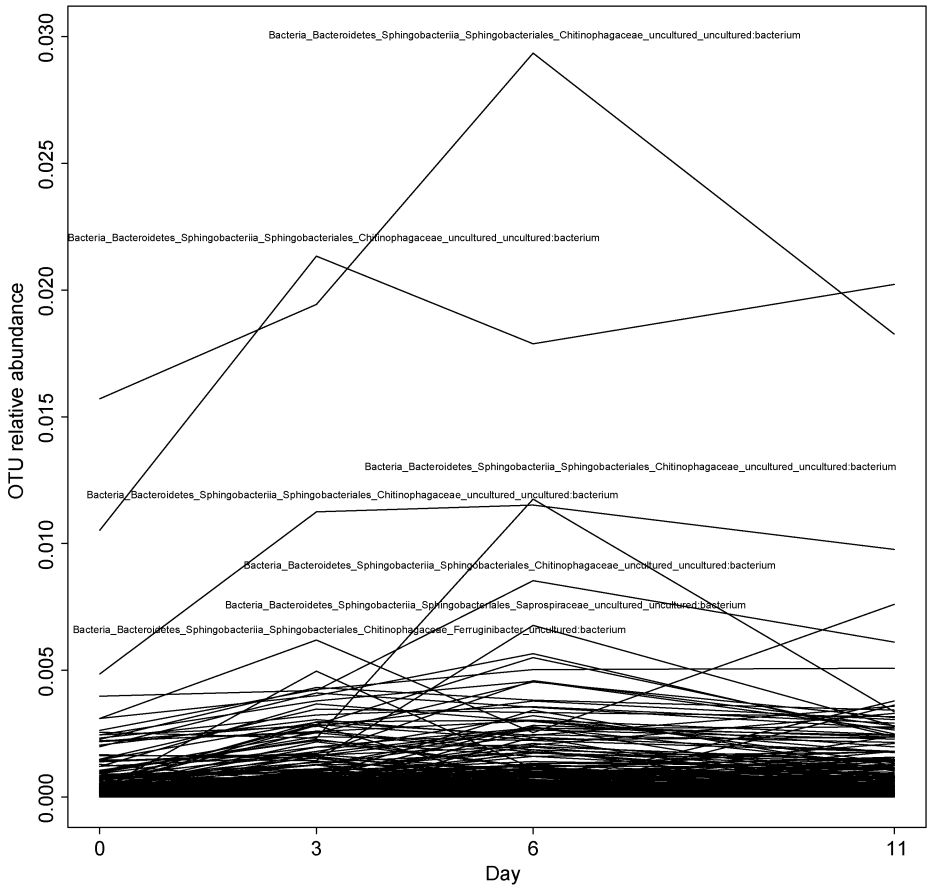

Figure S5 The change in abundance of OTU of the Sphingobacteriia taxa in Pi treatments.

Table S1 Soil physicochemical prosperities from the six study sites on the Fildes Peninsula

Site	Sample	Total organic carbon (TOC)/%	Total organic nitrogen (TON)/%	NH_4^+ -N /(μg·g^{-1})	SiO_3^{2-} -Si /(μg·g^{-1})	NO_3^- -N /(μg·g^{-1})	PO_4^{3-} -P /(μg·g^{-1})	NO_2^- -N /(μg·g^{-1})	Moisture content (MC)/%	pH	Day
S1	NPi0_S1	0.17	0.02	0.51	12.16	0.81	0.13	0.07	14.70	7.6	0
	NPi3_S1	0.18	0.03	0.33	13.15	0.62	0.18	0.07	15.69	7.59	3
	NPi6_S1	0.17	0.03	0.40	10.95	0.84	0.34	0.19	15.75	7.45	6
	NPi11_S1	0.13	0.03	0.50	11.12	0.78	0.28	0.13	11.79	7.54	11
S2	NPi0_S2	0.41	0.03	0.23	11.84	0.50	0.11	0.04	14.45	7.03	0
	NPi3_S2	0.01	0.03	0.29	6.70	0.72	0.09	0.04	11.76	7.17	3
	NPi6_S2	0.11	0.02	0.25	6.46	0.90	0.08	0.05	12.53	6.99	6
	NPi11_S2	0.09	0.04	0.34	5.95	0.67	0.12	0.06	13.25	6.89	11
S3	NPi0_S3	0.10	0.35	0.14	14.01	0.47	0.11	0.03	14.54	6.72	0
	NPi3_S3	0.05	0.41	0.16	10.09	0.62	0.21	0.05	16.00	6.43	3
	NPi6_S3	0.06	0.05	0.31	10.99	0.92	0.34	0.15	14.17	6.48	6
	NPi11_S3	0.06	0.03	0.28	11.03	0.59	0.14	0.06	15.95	6.73	11
S4	NPi0_S4	0.19	0.29	0.25	8.29	0.67	0.07	0.05	15.81	7.15	0
	Pi3_S4	0.10	0.03	0.25	11.49	0.80	0.35	0.04	16.38	7.09	3
	Pi6_S4	0.06	0.03	0.25	9.08	0.80	0.65	0.06	12.78	7.15	6
	Pi11_S4	0.07	0.03	0.40	10.16	0.78	0.50	0.10	13.74	7.11	11
S5	NPi0_S5	0.66	0.33	0.20	10.44	0.54	0.16	0.05	15.65	7.09	0

Continued

Site	Sample	Total organic carbon (TOC)/%	Total organic nitrogen (TON)/%	NH_4^+-N /(μg·g^{-1})	SiO_3^{2-}-Si /(μg·g^{-1})	NO_3^--N /(μg·g^{-1})	PO_4^{3-}-P /(μg·g^{-1})	NO_2^--N /(μg·g^{-1})	Moisture content (MC)/%	pH	Day
S5	Pi3_S5	0.11	0.38	0.41	5.47	0.89	0.27	0.04	11.74	7.23	3
	Pi6_S5	0.05	0.04	0.34	8.90	1.02	1.27	0.16	14.26	7.09	6
	Pi11_S5	0.15	0.03	0.24	9.11	0.65	0.51	0.10	13.78	7.01	11
S6	NPi0_S6	0.06	0.03	0.34	9.03	0.80	0.20	0.13	13.86	6.68	0
	Pi3_S6	0.04	0.27	0.24	7.07	0.79	0.26	0.06	13.32	6.9	3
	Pi6_S6	0.14	0.03	0.58	8.25	1.04	1.68	0.30	12.71	6.82	6
	Pi11_S6	0.12	0.02	0.20	8.00	0.86	0.87	0.05	13.26	6.81	11

Table S2 Summary data for Miseq sequencing data from the 12 samples in the present study

Sample ID	Raw_reads(#)	Effective/%	OTUs	ACE	Chao1	Shannon	Simpson	Coverage
NPi0_S1	52880	93.71	1848	2279.775	2309.188	5.938	0.0078	0.988
NPi0_S2	87477	91.69	1919	3522.102	3539.887	6.478	0.0040	0.980
NPi0_S3	75345	93.52	2248	3208.351	3905.265	6.196	0.0068	0.981
NPi0_S4	50919	86.5	1984	2320.199	2339.039	5.854	0.0135	0.988
NPi0_S5	50312	89.64	2637	2650.566	2634.516	6.390	0.0047	0.987
NPi0_S6	83022	96.62	2487	4189.066	3696.367	6.352	0.0053	0.978
NPi11_S1	51558	93.76	2840	2436.576	2501.430	6.194	0.0051	0.987
NPi11_S2	55490	90.13	2406	2862.751	2890.286	6.472	0.0041	0.986
NPi11_S3	59677	91.9	2394	2562.731	2434.798	6.446	0.0038	0.989
NPi3_S1	50329	89.85	2484	2322.035	2386.013	6.151	0.0055	0.988
NPi3_S2	64196	93.1	2649	2880.471	2739.029	6.510	0.0041	0.987
NPi3_S3	82226	97.47	2223	3308.543	3225.759	6.214	0.0065	0.981
NPi6_S1	72501	97	1884	3082.281	3545.196	6.268	0.0048	0.982
NPi6_S2	97363	96.17	2429	2787.642	2832.250	6.504	0.0038	0.986
NPi6_S3	89601	90.21	2612	3529.674	3558.518	6.445	0.0047	0.980
Pi11_S4	51386	93	2230	2734.514	2801.011	6.295	0.0051	0.986
Pi11_S5	59624	95.15	2224	2773.369	2647.058	6.547	0.0039	0.988
Pi11_S6	87351	90.18	2239	3653.880	3616.574	6.383	0.0045	0.978
Pi3_S4	82300	97.35	2631	3779.903	3303.989	6.328	0.0047	0.980
Pi3_S5	52632	85.62	2413	2661.411	2691.375	6.396	0.0047	0.987
Pi3_S6	82249	96.55	2642	3470.276	3489.157	6.407	0.0048	0.980
Pi6_S4	87477	91.42	2608	3559.228	3557.003	6.457	0.0042	0.979
Pi6_S5	86144	93.07	2249	3579.011	3652.200	6.410	0.0047	0.979
Pi6_S6	53681	94.31	2605	2645.768	2741.290	6.331	0.0056	0.987

Table S3 The naming system of the samples from the study sites for the LefSe analysis

Group	Sample	Day	phosphate
Group 1	NPi0_S1	0	No phosphate addition
	NPi0_S2	0	No phosphate addition
	NPi0_S3	0	No phosphate addition
	NPi0_S4	0	No phosphate addition
	NPi0_S5	0	No phosphate addition

Continued

Group	Sample	Day	phosphate
Group 1	NPi0_S6	0	No phosphate addition
Group 2	NPi3_S1	3	No phosphate addition
	NPi3_S2	3	No phosphate addition
	NPi3_S3	3	No phosphate addition
Group 3	NPi6_S1	6	No phosphate addition
	NPi6_S2	6	No phosphate addition
	NPi6_S3	6	No phosphate addition
Group 4	NPi11_S1	11	No phosphate addition
	NPi11_S2	11	No phosphate addition
	NPi11_S3	11	No phosphate addition
Group 5	Pi3_S4	3	Phosphate addition
	Pi3_S5	3	Phosphate addition
	Pi3_S6	3	Phosphate addition
Group 6	Pi6_S4	6	Phosphate addition
	Pi6_S5	6	Phosphate addition
	Pi6_S6	6	Phosphate addition
Group 7	Pi11_S4	11	Phosphate addition
	Pi11_S5	11	Phosphate addition
	Pi11_S6	11	Phosphate addition

Table S4 The most abundant taxa identified with network analysis in the controls and treatments

Hub nodes	NPi	Pi
d__Bacteria;p__Actinobacteria;c__Actinobacteria;o__Bifidobacteriales;f__Bifidobacteriaceae;g__Bifidobacterium	-	present
d__Bacteria;p__Actinobacteria;c__Actinobacteria;o__Frankiales;f__Geodermatophilaceae;g__Modestobacter	present	-
d__Bacteria;p__Actinobacteria;c__Actinobacteria;o__Micrococcales;f__Intrasporangiaceae;g__Oryzihumus	present	present
d__Bacteria;p__Actinobacteria;c__Actinobacteria;o__Micrococcales;f__Micrococcaceae;g__Pseudarthrobacter	present	-
d__Bacteria;p__Actinobacteria;c__Actinobacteria;o__Propionibacteriales;f__Nocardioidaceae;g__Nocardioides	present	-
d__Bacteria;p__Actinobacteria;c__Thermoleophilia;o__Gaiellales;f__Gaiellaceae;g__Gaiella	present	present
d__Bacteria;p__Armatimonadetes;c__Chthonomonadetes;o__Chthonomonadales;f__Chthonomonadaceae;g__Chthonomonas	present	present
d__Bacteria;p__Bacteroidetes;c__Bacteroidia;o__Bacteroidales;f__Prevotellaceae	-	present
d__Bacteria;p__Bacteroidetes;c__Flavobacteriia;o__Flavobacteriales;f__Flavobacteriaceae;g__Flavobacterium	present	present
d__Bacteria;p__Bacteroidetes;c__Sphingobacteriia;o__Sphingobacteriales;f__Chitinophagaceae	present	present
d__Bacteria;p__Bacteroidetes;c__Sphingobacteriia;o__Sphingobacteriales;f__Chitinophagaceae;g__Ferruginibacter	present	present
d__Bacteria;p__Bacteroidetes;c__Sphingobacteriia;o__Sphingobacteriales;f__Chitinophagaceae;g__Sediminibacterium	present	-
d__Bacteria;p__Bacteroidetes;c__Sphingobacteriia;o__Sphingobacteriales;f__Sphingobacteriaceae;g__Pedobacter	present	present
d__Bacteria;p__Chloroflexi;c__Chloroflexia;o__Chloroflexales;f__Roseiflexaceae;g__Roseiflexus	present	present
d__Bacteria;p__Firmicutes;c__Bacilli;o__Bacillales;f__Bacillaceae	present	present
d__Bacteria;p__Gemmatimonadetes;c__Gemmatimonadetes;o__Gemmatimonadales;f__Gemmatimonadaceae;g__Gemmatimonas	present	present
d__Bacteria;p__Proteobacteria;c__Alphaproteobacteria;o__Rhodobacterales;f__Rhodobacteraceae;g__Pseudorhodobacter	present	-
d__Bacteria;p__Proteobacteria;c__Alphaproteobacteria;o__Rhodospirillales;f__Acetobacteraceae	-	present
d__Bacteria;p__Proteobacteria;c__Alphaproteobacteria;o__Sphingomonadales;f__Sphingomonadaceae;g__Novosphingobium	present	present
d__Bacteria;p__Proteobacteria;c__Alphaproteobacteria;o__Sphingomonadales;f__Sphingomonadaceae;g__Sphingomonas	-	present
d__Bacteria;p__Proteobacteria;c__Gammaproteobacteria;o__Enterobacteriales;f__Enterobacteriaceae;g__Klebsiella	-	present

Continued

Hub nodes	NPi	Pi
d__Bacteria;p__Proteobacteria;c__Gammaproteobacteria;o__Enterobacteriales;f__Enterobacteriaceae;g__Serratia	-	present
d__Bacteria;p__Proteobacteria;c__Gammaproteobacteria;o__Pseudomonadales;f__Moraxellaceae;g__Alkanindiges	present	-
d__Bacteria;p__Proteobacteria;c__Gammaproteobacteria;o__Xanthomonadales;f__Xanthomonadaceae	present	-
d__Bacteria;p__Proteobacteria;c__Gammaproteobacteria;o__Xanthomonadales;f__Xanthomonadaceae;g__Lysobacter	present	-
d__Bacteria;p__Proteobacteria;c__Gammaproteobacteria;o__Xanthomonadales;f__Xanthomonadaceae;g__Stenotrophomonas	present	present